Published in final edited form as:
Acta Radiol. 2009 December ; 50(10): 1095–1103. doi:10.3109/02841850903008800.

Characterizing Breast Cancer Xenograft Epidermal Growth Factor Receptor Expression by Using Near-Infrared Optical Imaging

Kezheng Wang[1,*], **Kai Wang**[1,*], **Weihual Li**[1], **Tao Huang**[1], **Renfei Li**[1], **Dan Wang**[1], **Baozhong Shen**[1], and **Xiaoyuan Chen**[2]

[1]Department of Medical Imaging and Nuclear Medicine, Fourth Affiliated Hospital, Harbin Medical University, Harbin, China

[2]Department of Radiology, Bio-X & Biophysics, Stanford University School of Medicine, Stanford, California, USA

Abstract

Background—Epidermal growth factor receptor (EGFR) overexpression is associated with several key features of cancer development and growth. Therefore, EGFR is a very promising biological target for tumor diagnosis and anticancer therapy. Characterization of EGFR expression is important for clinicians to select patients for EGFR-targeted therapy and evaluate therapeutic effects.

Purpose—To investigate whether near-infrared (NIR) fluorescent dye Cy5.5-labeled anti-EGFR monoclonal antibody Erbitux can characterize EGFR expression level in MDA-MB-231 and MCF-7 breast cancer xenografts using an in vivo NIR imaging method.

Material and Methods—A fluorochrome probe was designed by coupling Cy5.5 to Erbitux through acidylation, and the fluorescence property of the Erbitux-Cy5.5 conjugate was characterized by fluorospectroscopy. Flow cytometry and laser confocal microscopy were used to test the EGFR specificity of the antibody probe in vitro. Erbitux-Cy5.5 was also injected intravenously into immune-deficient mice bearing MDA-MB-231 or MCF-7 tumors. Whole-body and region-of-interest fluorescence images were acquired and analyzed. The EGFR expression was also analyzed and confirmed by immunohistochemical assay.

Results—The maximum excitation/emission wavelength for the Erbitux-Cy5.5 probe was 674/697 nm, similar to that of free Cy5.5 (674/712 nm). Confocal microscopy confirmed receptor-specific uptake in MDA-MB-231 and MCF-7 cells. In flow cytometry probe specificity assay, Erbitux-Cy5.5 showed a 9.32-fold higher affinity for MDA-MB-231 than MCF-7 cells. In vivo NIR imaging also indicated specific uptake in EGFR-positive tumors. Probe uptake rate and maximum intake dose in MDA-MB-231 were significantly higher than those in MCF-7 xenografts ($P < 0.001$). Immunohistochemical staining confirmed the in vivo imaging results, showing differentiated EGFR expression in MDA-MB-231 (+ + +) and MCF-7 (+) tumor tissues.

Conclusion—Erbitux-Cy5.5 may be used as a specific NIR contrast agent for the noninvasive characterization of EGFR expression level in breast cancer xenografts.

Baozhong Shen, Department of Medical Imaging and Nuclear Medicine, Harbin Medical University, Yiyuan Street 135, Nan gang District, Harbin, China, 150001 (tel. +86 451 82576508, fax. +86 451 82576509, baozhongshen@gmail.com).
*These authors contributed equally to the work.

Declaration of interest: The authors report no conflicts of interest. The authors alone are responsible for the content and writing of the paper.

Keywords

Anti-EGFR monoclonal antibody; breast cancer; epidermal growth factor receptor (EGFR); molecular imaging; near-infrared optical imaging

Epidermal growth factor receptor (EGFR, HER1) over-expression has been believed to be one of the processes by which cancer cells acquire the ability to escape normal growth regulatory mechanisms (1) and has been observed in 35–70% of human breast cancers (2, 3). Epidermal growth factor (EGF) is a 6-kDa polypeptide that binds to a 170-kDa cell surface receptor EGFR, which is a transmembrane glycoprotein with an intracellular tyrosine kinase domain. The ligand binding results in the erbB receptors (HER1, HER2, HER3, HER4) to form homodimers or heterodimers, causing the activation of the EGFR tyrosine kinase, which in turn activates the mitogen-activated protein kinase and kinase signaling pathways, and finally leads to cell proliferation, differentiation, angiogenesis, invasion and metastasis, as well as motility and survival (4, 5). Meanwhile, EGFR overexpression in breast cancer is inversely correlated with estrogen receptor (ER) expression and is directly correlated with advanced tumor stage, resistant to standard therapies (hormonal therapy, chemotherapy, and radiation) (6–9). Therefore, abnormalities and dysfunction of EGFR are involved in various aspects of carcinogenesis and tumor progression (10), and consequently EGFR becomes an excellent target for diagnosis and anti-tumor therapy (11, 12). EGFR-targeted therapeutic agents, including specific antibodies directed against its ligand-binding domain and small molecules inhibiting its tyrosine kinase activity, are either under clinical trial or have already been approved for clinical treatment (4, 9, 11, 13). However, there are few reliable methods to monitor the intended target (e.g., EGFR expression) and predict the response to therapy or gauge treatment response over time (14), which is a major hindrance to further developing these specifically targeted and highly efficient therapies.

Noninvasive imaging techniques for measuring tumor physiologic parameters on the molecular level are being developed (15), which may facilitate repetitive and quantitative imaging of EGFR before or during a course of treatment. As new cancer therapeutic agents more specifically target tumor cell signaling pathways, such molecular imaging technology is becoming increasingly important (16). Pretreatment targeted imaging of particular molecules could be used to help physicians to identify patients who are likely to benefit from targeted therapies. During the course of treatment, receptor-specific imaging could also assist early assessment of therapeutic target inhibition before alterations in tumor size become apparent (17).

Among the different imaging technologies being used to display molecular events, near-infrared (NIR) fluorescence optical imaging, using neither ionizing radiation nor radioactive materials, is particularly promising (18). Although depth penetration is one major limiting factor for in vivo optical imaging, the tissue penetration of light is substantially increased (from millimeters to centimeters) using NIR probes, as the absorption by water and hemoglobin is relatively low in the NIR spectral window (650–900-nm “diagnostic window”) (19). Thus, it enables the imaging of tumors within tissue, such as breast tissue (17). NIR fluorescent dye Cy5.5 has proven to be a promising contrast agent for the in vivo demarcation of tumors by several groups (17, 20–23). Here, we chose the widely used Cy5.5 dye for our optical imaging studies. Erbitux was the first FDA-approved anti-EGFR monoclonal antibody drug with anticancer activity on the market (24). It selectively binds to the external domain of the receptor with affinity comparable to the natural ligand (K_d = 1 nM) and competes with EGF binding (23).

The aim of this study was to investigate whether in vivo NIR fluorescence imaging mediated by an Erbitux-Cy5.5 conjugate could be used to discriminate EGFR expression level in nude mice models implanted with EGFR-overexpressing, estrogen-independent, highly invasive, and metastatic human breast MDA-MB-231 cells and low-EGFR-expressing, estrogen-dependent, poorly invasive, and non-metastatic MCF-7 cells, each of which represents a clinically relevant subtype of human breast cancer (25, 26).

Material and Methods

Fluorochrome probe generation

Cy5.5 dye molecules with monofunctional *N*-hydroxysuccinimide (NHS) ester (Cy5.5-NHS; GE Healthcare, Piscataway, N.J., USA) were coupled to Erbitux (ImClone Systems, Branchburg, N.J., USA) according to a protocol from the previous literature, with modifications (22). Briefly, Erbitux (10 mg, 66.7 nmol) dissolved in 500 μl of 0.1 mol/l sodium borate ($Na_2B_4O_7$) buffer (pH 8.3) was mixed with Cy5.5-NHS (0.4 mg, 355 nmol) in H_2O (100 μl) in the dark at 4°C. After stirring for 2 hours in the dark at 4°C, the reaction was quenched by adding 100 μl of 5% acetic acid (HOAc). The labeled antibody was isolated by a PD-10 disposable column (GE Healthcare, Piscataway, N.J., USA). The peak containing the Erbitux-Cy5.5 conjugate was collected, lyophilized, and re-dissolved in saline at a concentration of 1 mg/ml, and stored in the dark at −20°C until use. To measure and characterize the absorption and emission spectra of Erbitux-Cy5.5, identical dye concentrations of Erbitux-Cy5.5 and Cy5.5 were put in a quartz pool. Maximum absorption and emission wavelengths were determined in the scope of 200–800 nm, under a Cary-Eclipse 4000 ultraviolet-visible light fluorospectrophotometer (Varian, Inc., Palo Alto, Calif., USA).

Cell culture

Human breast cancer cells that express a high level of EGFR (MDA-MB-231) and a low level of EGFR (MCF-7) were obtained from the China Science Institute Cell Bank (Shanghai, China) and cultured, following the instructions from the American Type Culture Collection (ATCC). Briefly, MDA-MB-231 cells were cultured in Leibovitz's L-15 medium (Invitrogen, Carlsbad, Calif., USA), while MCF-7 cells were cultured in Dulbecco's minimum essential medium (DMEM; Sigma Chemical Co., St. Louis, Mo., USA), with 10% fetal bovine serum (FBS; Gibco BRL, Cleveland, Ohio, USA), 100 U penicillin, 0.1 μg streptomycin, and 2 mmol/l L-glutamax, in an humidified incubator maintained at 37°C with 5% CO_2.

In vitro receptor binding studies

The binding of Erbitux-Cy5.5 to EGFR was assessed by using flow cytometry. Briefly, 2×10^6 MDA-MB-231 and 2×10^6 MCF-7 cells were incubated in suspension with 5 nM Erbitux-Cy5.5 for 30 min at 37°C in a total volume of 150 μl, respectively, protected from light and then centrifugally elutriated twice in phosphate buffered solution (PBS, pH 7.2, 10 mM). Fluorescence intensity was assessed with flow cytometry (FACSort; Becton Dickinson, Franklin Lakes, N.J., USA). For competitive inhibition of probe binding, 5-nM-labeled probes, along with 500 nM of Erbitux, were added to the MDA-MB-231 and MCF-7 cells, respectively, by using the same incubation and washing conditions, followed by flow cytometric analysis. As the blank control, PBS was added to each assay group. All experiments were carried out in triplicate, and the mean values were calculated. Fluorescence microscopy (with an Olympus confocal microscope outfitted with NIR diode sources and filters) of probe-stained tumor cells and the specific antibody block experiment were also performed for visual confirmation of the intake of Erbitux-Cy5.5 in MDA-MB-231 and MCF-7 cells. DAPI was used to stain cell nuclei. In the microscopic images,

Erbitux-Cy5.5 was pseudo-colored red (emission at 680–710 nm), while DAPI was pseudocolored blue (emission at 461 nm).

Tumor xenografts

All mouse studies were conducted in accordance with an Institute of Animal Care and Use Committee (IACUC)-approved protocol. Female athymic nude mice (BALB/c-nu/nu, 4–6 weeks old, 18–22 g) from Vital River Laboratories (National Science Institute, Beijing, China) were housed five per cage and provided with sterilized pellet chow and sterilized water. Animals were maintained in a pathogen-free mouse colony at the Tumor Treatment and Prevention Institute (TTPI) at the Harbin Medical University (Harbin, China). MDA-MB-231 and MCF-7 cells were treated with trypsin when near confluence and harvested. Cells were centrifuged at 1200 rpm for 5 min and re-suspended in sterile culture medium. The suspension (5×10^6 cells/0.2 ml) was injected into the mouse left chest mammary gland fat pad. When the tumors reached 0.4 to 0.6 cm in diameter (14–21 days after implant), the tumor-bearing mice were subjected to in vivo imaging studies.

In vivo optical imaging system

The mice were imaged with an eXplore Optix time-domain fluorescence imaging system (ART/GE Healthcare, Saint-Laurent, Quebec, Canada) to detect Erbitux-Cy5.5 in tumors, which was a temperature-controlled, light-tight box with a cryogenically cooled back-illuminated digital charge-coupled device (CCD) camera. The system featured a 667-nm pulse laser for excitation, with a 710-nm bandpass filter on the emission side. Image acquisition was accomplished using time-domain Molecular Imager software, and the obtained images were stored in the bmp image file format. All image stacks were acquired by using identical laser power (2 μW), integration time (1 s/point), resolution rate, window, and level settings. Data processing and analysis was accomplished using eXplore OPTX-optView software (ART/GE Healthcare, Saint-Laurent, Quebec, Canada).

In vivo NIR optical imaging

For in vivo testing of the specificity of Erbitux-Cy5.5, mice bearing MDA-MB-231 ($n = 5$) and MCF-7 tumors ($n = 5$) were anesthetized with an intraperitoneal (i.p.) injection of 50 mg/kg pentobarbital and then intravenously (i.v.) injected with 0.2 nmol per mouse Erbitux-Cy5.5 via the tail vein. For the blocking study, 3 mg of Erbitux (20 nmol, 100-fold excess) was injected i.v. to each MDA-MB-231 ($n = 5$) or MCF-7 mouse ($n = 5$) 24 hours prior to the injection of 0.2 nmol Erbitux-Cy5.5. Whole-body fluorescence images were then acquired every 30 min up to 6 hours post injection, and each mouse was imaged again at the 24-hour time point. At the end of the imaging studies, ex vivo fluorescence images of the dissected tumor tissue and organs were obtained.

To observe the tumor clearance pattern of Erbitux-Cy5.5 in vivo, dynamic scans were acquired. Briefly, MDA-MB-231 ($n = 5$) and MCF-7 mice ($n = 5$) were anesthetized with i.p. injection of pentobarbital and then i.v. injected with Erbitux-Cy5.5 (0.2 nmol/mouse). By using the white-light image as a guide, symmetric tumor and normal regions of interest (ROI) were designated in each mouse chest part. The local ROI imaging was performed every 10 min up to 6 hours post injection, and from 24 to 192 hours at intervals of every 24 hours.

EGFR immunohistochemical (IHC) analysis

The immunohistochemistry for EGFR staining was determined by a two-step method. Formalin-fixed, paraffin-embedded tissue blocks were obtained from MDA-MB-231 and MCF-7 xenografts. Five-μm-thick tissue sections were cut, de-waxed, microwave pre-

treated, and incubated with 0.3% hydrogen peroxide in methanol for 30 min. After blocking to reduce nonspecific antibody binding, monoclonal rabbit anti-human EGFR antibody (1:150, COOH terminus; Santa Cruz Biotechnology, Santa Cruz, Calif., USA) was reacted with tissue sections at room temperature for 2 hours, followed by three washes with PBS. The sections were incubated with goat anti-rabbit IgG (Southern Biotechnology Associates, Birmingham, Ala., USA), and then reacted with streptoavidin-biotin peroxidase reagent (Histofine kit; Nichirei Biosciences Inc., Tokyo, Japan). Finally, diaminobenzidine (DAB) and 1% hydrogen peroxidase were applied as chromogen, counterstained with hematoxylin.

Statistical analysis

Standardized fluorescence values were calculated by dividing the fluorescence within the ROI by the value of the ROI area. Data were presented as means ± standard deviation. The mean value from each ROI was plotted as a function of time for up to 192 hours post injection. Statistical significance was assessed by using repeated-measures analysis of variance to compare the mean fluorescence values binding in different tumor and normal-tissue ROIs at different time points post injection. Independent (or adjusted independent) samples Student *t* test was used to compare the mean fluorescence intensities of other measurement data. Nonparametric test (Mann-Whitney test) was used to compare the difference of IHC results. A statistical software package (SPSS 13.0; SPSS, Inc., Chicago, Ill., USA) was used for data analysis. Statistical significance was assigned for *P* values ± 0.05.

Results

Synthesis and characterization of fluorochrome probe

Cy5.5 has a degree of labeling of 4.2 mol of dye per mole of protein, and the yield of the Erbitux-Cy5.5 conjugate was typically 68–70%, as calculated with $\varepsilon_{678\ nm} = 250{,}000\ M^{-1}cm^{-1}$. The excitation and emission wave spectra showed that the maximum excitation/emission wavelengths for the Erbitux-Cy5.5 conjugate were 674/697 nm and for Cy5.5 were 674/712 nm, suggesting that the fluorescence property of Cy5.5 was not affected by conjugation to Erbitux.

In vitro probe binding studies by flow cytometry and confocal microscopy

The Erbitux-Cy5.5 probe showed a 9.3-fold increase in binding to MDA-MB-231 compared with MCF-7 cells (Fig. 1A). As measured according to fluorescence intensity counts, the mean gated percentage of MDA-MB-231 was 69.0 ± 2.5%, while MCF-7 was 7.4 ± 1.8% ($n = 3$, $P < 0.001$). At competitive receptor binding assay, probe binding was competitively inhibited by the addition of a 100-fold molar excess of unlabeled Erbitux in MDA-MB-231 and MCF-7 cells. Fluorescence microscopy of probe-stained MDA-MB-231 and MCF-7 tumor cells (Fig. 1B, first and third rows) confirmed the probe uptake to the cell endochylema. More intense cellular fluorescence signal was observed in MDA-MB-231 cells than in MCF-7 cells, which is consistent with the higher levels of EGFR expression in MDA-MB-231 cells. Furthermore, the binding of the probe was completely blocked by anti-EGFR antibody Erbitux (100-fold excess, Fig. 1B, second and fourth rows). These results further confirmed that the receptor binding affinity and specificity of Erbitux in vitro was not affected by the conjunction.

In vivo fluorescence imaging

Typical whole-body NIR fluorescence images of athymic nude mice bearing orthotopic transplanted MDA-MB-231 and MCF-7 breast tumors verified that the fluorescent probe specifically accumulated in tumor regions 24 hours after intravenous injection (Fig. 2). The

mean fluorescence intensity in the tumor was 30,218 ± 6583 arbitrary units (au) for MDA-MB-231 ($n = 5$) and 18,908 ± 1771 au for MCF-7 ($n = 5$). To validate that the tumor accumulation of the fluorescent dye complex was receptor specific, a blocking experiment was performed. An excess amount of Erbitux successfully reduced tumor contrast. The MDA-MB-231 tumor region mean fluorescence intensity was 10,470 ± 838 au ($n = 5$, $P = 0.002$), and that for MCF-7 was 9058 ± 795 au ($n = 5$, $P < 0.001$). Although the pretreatment with Erbitux resulted in a significant decrease of tumor uptake of Erbitux-Cy5.5, the tumor accumulation was not completely blocked even with a higher dose of unlabeled Erbitux. The residual contrast is likely due to some nonspecific binding accumulated in the extra-cellular space; similar findings have also been reported elsewhere (22).

To fully characterize the clearance pattern of Erbitux, the fluorescence intensities in the tumor and the normal tissue were measured dynamically after the injection of Erbitux-Cy5.5 in MDA-MB-231 and MCF-7 tumor-bearing mice (Fig. 3). The mean fluorescence intensities in the ROIs of MDA-MB-231 and MCF-7 tumors were significantly higher than in normal area, which varied with time ($n = 5$, $P < 0.001$). In the MDA-MB-231 model, the maximum probe uptake fluorescence intensity occurred at 4 hours post injection (39,000 ± 1343 au) (Fig. 3B), while in the MCF-7 model, the maximum probe uptake fluorescence intensity occurred at 6 hours post injection (23,592 ± 1673 au) and plateaued up to 72 h before being cleared out (Fig. 3D). The maximum probe uptake was 1.65-fold higher in the MDA-MB-231 tumor than in the MCF-7 tumor ($P < 0.001$). The different slope rates indicated that the average probe uptake rate in the MDA-MB-231 tumors (Fig. 3B) was higher than in the MCF-7 tumors (Fig. 3D).

EGFR IHC analysis

Upregulation of EGFR in the tumor region, relative to normal surrounding tissues, permits the preferential delivery of suitably labeled EGFR ligand to the receptor-positive tumors. IHC assays were carried out to correlate the magnitude of tumor uptake (signal brightness) with the tumor receptor density distribution. IHC staining results (Fig. 4) showed that the MDA-MB-231 tumor was highly EGFR positive (+ + +, $n = 5$), whilst the MCF-7 tumor had relatively low expression (+, $n = 5$, $P = 0.004$). These observations were consistent with the in vitro and in vivo fluorescence measurements.

Discussion

In the present study, we investigated the feasibility of using Erbitux-Cy5.5 as a probe for noninvasive optical imaging and characterization of EGFR expression in human breast cancer xenografts in mice. Our findings demonstrated the specific targeting of Erbitux-Cy5.5 to EGFR both in vitro and in vivo. In addition, our results also indicated that the maximum probe uptake rate and maximum fluorescence intensity in the MDA-MB-231 tumors ($n = 5$) was higher than in the MCF-7 tumors, which correlated well with the receptor density measured by the ex vivo immunohistochemical analysis.

Because of its high sensitivity and spatial resolution, optical imaging technology with cancer-specific contrast agent is a rapidly burgeoning imaging modality with high clinical potential (17, 21, 22, 27, 28). It has the potential to provide noninvasive insight into the pathophysiologic features and metastasis status of tumors for physicians (17) and surgeons (23, 28), and to aid in initial tumor characterization and determination of therapy response, which will be particularly important in patients undergoing molecularly targeted cancer therapy. As mentioned above, it is important for physicians to identify whether the target molecule (e.g., EGFR) is highly expressed in the patients and whether they would benefit from the targeted therapy (e.g., EGFR inhibition) before and during the treatment. In case of no tumor size reduction, it is critical to know whether the lack of response is due to

inadequate drug delivery or therapeutic resistance, which may need an increase of dosage or the alteration of therapeutic regimen (17). In addition, as used in this study, if we could couple the fluorescent dye to targeted therapeutic agents, the ability to assess the kinetics of the targeted agent in vivo would expedite the process of optimal therapy dosing in individual patients for a maximized therapeutic effect while minimizing drug toxicity (29).

Fluorescence imaging is readily applicable to human breast tumor evaluation because diffuse optical tomography and spectroscopy with NIR light are currently being evaluated in clinical studies to distinguish the benign from malignant breast lesions and follow tumor response to chemotherapy (30–32). However, we have to admit that several obstacles exist for the clinical translation of Erbitux-Cy5.5. Although Erbitux is FDA approved for use in humans, the fluorophore Cy5.5 is not. ICG is similar in molecular structure and is used in gram quantities in humans, without known toxicity. Unfortunately, ICG cannot be easily conjugated to proteins, and it does not offer the fluorescence intensity of Cy5.5. The approval of a fluorescent marker that provides intense fluorescence, although posing no toxic hazard to the patient, is imperative to facilitate clinical experimentation (28). Because this was a pilot study to demonstrate the feasibility of the imaging technique for characterizing EGFR expression level in vivo, a relatively small number of mice and animal models were used.

Confocal microscopy indicated that the fluorescence signal was observed in the cytoplasmic region, which may be attributed to the internalization of Erbitux-Cy5.5. As reported recently (33), rapid receptor internalization through circular dorsal ruffles in plasma membrane may explain why prolonged incubation time may result in endocytosis and internalization, which brought the fluorescent probes into the cytoplasm and accumulated in the perinuclear region. The internalization of the probes in the cytoplasmic region may also explain the reason why the fluorescence signals still can be detected in tumors up to 96 hours post injection of the fluorescent probe without washing out during in vivo NIR imaging studies.

It is interesting to speculate on the reasons why we merely observed an indirect quantitative relationship between in vitro probe binding level and in vivo accumulation level of fluorescent probes in the corresponding breast cancer xenografts. Besides the difference of EGFR expression level on the tumor cell surface, another possible reason might be that, in the context of tumor-bearing mice, EGFR is ubiquitously expressed in normal tissues (such as liver, kidney, muscles, tumor-adjacent normal tissues), albeit at a much lower level than on tumors, and it is likely that only small concentrations of the fluorescent probes actually reached the interstitial fluid bathing the cancer cells after blood circulation. Another factor in the different binding capacities of these tumors may be the differences in the tumor cell sizes. MCF-7 cells are smaller than MDA-MB-231 cells, and for a tumor of a given size, there are a higher number of MCF-7 cells with a higher surface-area-to-volume ratio. Different cancer cell morphology and tissue structure of the two tumors result in the diverse vascular permeability, blood vessel density, and hydrostatic pressure, which may also affect probe delivery to the targets.

In conclusion, this Erbitux-Cy5.5 probe with favorable binding affinity to EGFR permits quantifiable imaging of EGFR expression in breast cancer xenografts in mice models. Although near-infrared contrast agents are still in the experimental stage, once the concerns about the toxicity and optimization of these probes have been addressed, this class of probes could have potential clinical application, including early detection of cancers (primary, recurrent, or metastatic), image-guided receptor-targeted sentinel node biopsies, treatment monitoring, customized dose optimization of targeted therapy, and accelerated drug screening and development.

Acknowledgments

This work was supported, in part, by the National Natural Science Foundation of China (30570527), the Doctoral Workstation Foundation Grants of Education Ministry of China (20050226016), and the Heilongjiang Province Excellent Youth Foundation Grant (JC2005-04).

References

1. Reilly RM, Kiarash R, Sandhu J, Lee YW, Cameron RG, Hendler A, et al. A comparison of EGF and MAb 528 labeled with ^{111}In for imaging human breast cancer. J Nucl Med. 2000; 41:903–11. [PubMed: 10809207]
2. Klijn JG, Berns PM, Schmitz PI, Foekens JA. The clinical significance of epidermal growth factor receptor (EGF-R) in human breast cancer: a review on 5232 patients. Endocr Rev. 1992; 13:3–17. [PubMed: 1313356]
3. Ciardiello F, Tortora G. Anti-epidermal growth factor receptor drugs in cancer therapy. Expert Opin Investig Drugs. 2002; 11:755–68.
4. Baselga J. Targeting tyrosine kinases in cancer: the second wave. Science. 2006; 312:1175–8. [PubMed: 16728632]
5. Blume-Jensen P, Hunter T. Oncogenic kinase signalling. Nature. 2001; 411:355–65. [PubMed: 11357143]
6. Sartor CI. Biological modifiers as potential radiosensitizers: targeting the epidermal growth factor receptor family. Semin Oncol. 2000; 27:15–20. [PubMed: 11236022]
7. Newby JC, Johnston SR, Smith IE, Dowsett M. Expression of epidermal growth factor receptor and c-erbB2 during the development of tamoxifen resistance in human breast cancer. Clin Cancer Res. 1997; 3:1643–51. [PubMed: 9815855]
8. Agrawal A, Gutteridge E, Gee JM, Nicholson RI, Robertson JF. Overview of tyrosine kinase inhibitors in clinical breast cancer. Endocr Relat Cancer. 2005; 12(Suppl 1):S135–44. [PubMed: 16113090]
9. Arteaga CL. Overview of epidermal growth factor receptor biology and its role as a therapeutic target in human neoplasia. Semin Oncol. 2002; 29(Suppl 14):3–9. [PubMed: 12422308]
10. Wujcik D. EGFR as a target: rationale for therapy. Semin Oncol Nurs. 2006; 22(Suppl 1):5–9. [PubMed: 16616281]
11. Baselga J, Arteaga CL. Critical update and emerging trends in epidermal growth factor receptor targeting in cancer. J Clin Oncol. 2005; 23:2445–59. [PubMed: 15753456]
12. Laskin JJ, Sandler AB. Epidermal growth factor receptor: a promising target in solid tumours. Cancer Treat Rev. 2004; 30:1–17. [PubMed: 14766123]
13. Harris M. Monoclonal antibodies as therapeutic agents for cancer. Lancet Oncol. 2004; 5:292–302. [PubMed: 15120666]
14. Arteaga CL. Epidermal growth factor receptor dependence in human tumors: more than just expression? Oncologist. 2002; 7:31–9. [PubMed: 12202786]
15. Rudin M, Weissleder R. Molecular imaging in drug discovery and development. Nat Rev Drug Discov. 2003; 2:123–31. [PubMed: 12563303]
16. Chabner BA, Roberts TG Jr. Timeline: chemotherapy and the war on cancer. Nat Rev Cancer. 2005; 5:65–72. [PubMed: 15630416]
17. Gee M, Upadhyay R, Bergquist H, Alencar H, Reynolds F, Maricevich M, et al. Human breast cancer tumor models: molecular imaging of drug susceptibility and dosing during HER2/neu-targeted therapy. Radiology. 2008; 248:925–35. [PubMed: 18647846]
18. Weissleder R. Molecular imaging in cancer. Science. 2006; 312:1168–71. [PubMed: 16728630]
19. Weissleder R. A clearer vision for in vivo imaging. Nat Biotechnol. 2001; 19:316–7. [PubMed: 11283581]
20. Ke S, Wen X, Gurfinkel M, Charnsangavej C, Wallace S, Sevick-Muraca E, et al. Near-infrared optical imaging of epidermal growth factor receptor in breast cancer xenografts. Cancer Res. 2003; 63:7870–5. [PubMed: 14633715]

21. Hsu AR, Hou LC, Veeravagu A, Greve JM, Vogel H, Tse V, et al. In vivo near-infrared fluorescence imaging of integrin αvβ3 in an orthotopic glioblastoma model. Mol Imaging Biol. 2006; 8:315–23. [PubMed: 17053862]
22. Chen X, Conti PS, Moats RA. In vivo near-infrared fluorescence imaging of integrin αvβ3 in brain tumor xenografts. Cancer Res. 2004; 64:8009–14. [PubMed: 15520209]
23. Rosenthal EL, Kulbersh BD, King T, Chaudhuri TR, Zinn KR. Use of fluorescent labeled anti-epidermal growth factor receptor antibody to image head and neck squamous cell carcinoma xenografts. Mol Cancer Ther. 2007; 6:1230–8. [PubMed: 17431103]
24. Harding J, Burtness B. Cetuximab: an epidermal growth factor receptor chemeric human-murine monoclonal antibody. Drugs Today (Barc). 2005; 41:107–27. [PubMed: 15821783]
25. Li H, Weinstein IB. Protein kinase C β enhances growth and expression of cyclin D1 in human breast cancer cells. Cancer Res. 2006; 66:11399–408. [PubMed: 17145886]
26. Jang BC, Sanchez T, Schaefers HJ, Trifan OC, Liu CH, Creminon C, et al. Serum withdrawal-induced post-transcriptional stabilization of cyclooxygenase-2 mRNA in MDA-MB-231 mammary carcinoma cells requires the activity of the p38 stress-activated protein kinase. J Biol Chem. 2000; 275:39507–15. [PubMed: 10993880]
27. Veiseh M, Gabikian P, Bahrami SB, Veiseh O, Zhang M, Hackman RC, et al. Tumor paint: a chlorotoxin:Cy5. 5 bio-conjugate for intraoperative visualization of cancer foci. Cancer Res. 2007; 67:6882–8. [PubMed: 17638899]
28. Gleysteen JP, Newman JR, Chhieng D, Frost A, Zinn KR, Rosenthal EL. Fluorescent labeled anti-EGFR antibody for identification of regional and distant metastasis in a preclinical xenograft model. Head Neck. 2008; 30:782–9. [PubMed: 18228526]
29. Kaijzel EL, van der Pluijm G, Löwik CW. Whole-body optical imaging in animal models to assess cancer development and progression. Clin Cancer Res. 2007; 13:3490–7. [PubMed: 17575211]
30. Choe R, Corlu A, Lee K, Durduran T, Konecky SD, Grosicka-Koptyra M, et al. Diffuse optical tomography of breast cancer during neoadjuvant chemotherapy: a case study with comparison to MRI. Med Phys. 2005; 32:1128–39. [PubMed: 15895597]
31. Spinelli L, Torricelli A, Pifferi A, Taroni P, Danesini G, Cubeddu R. Characterization of female breast lesions from multi-wavelength time-resolved optical mammography. Phys Med Biol. 2005; 50:2489–502. [PubMed: 15901950]
32. Tromberg BJ, Cerussi A, Shah N, Compton M, Durkin A, Hsiang D, et al. Imaging in breast cancer: diffuse optics in breast cancer: detecting tumors in pre-menopausal women and monitoring neoadjuvant chemotherapy. Breast Cancer Res. 2005; 7:279–85. [PubMed: 16457705]
33. Orth JD, McNiven MA. Get off my back! Rapid receptor internalization through circular dorsal ruffles. Cancer Res. 2006; 66:11094–6. [PubMed: 17145849]

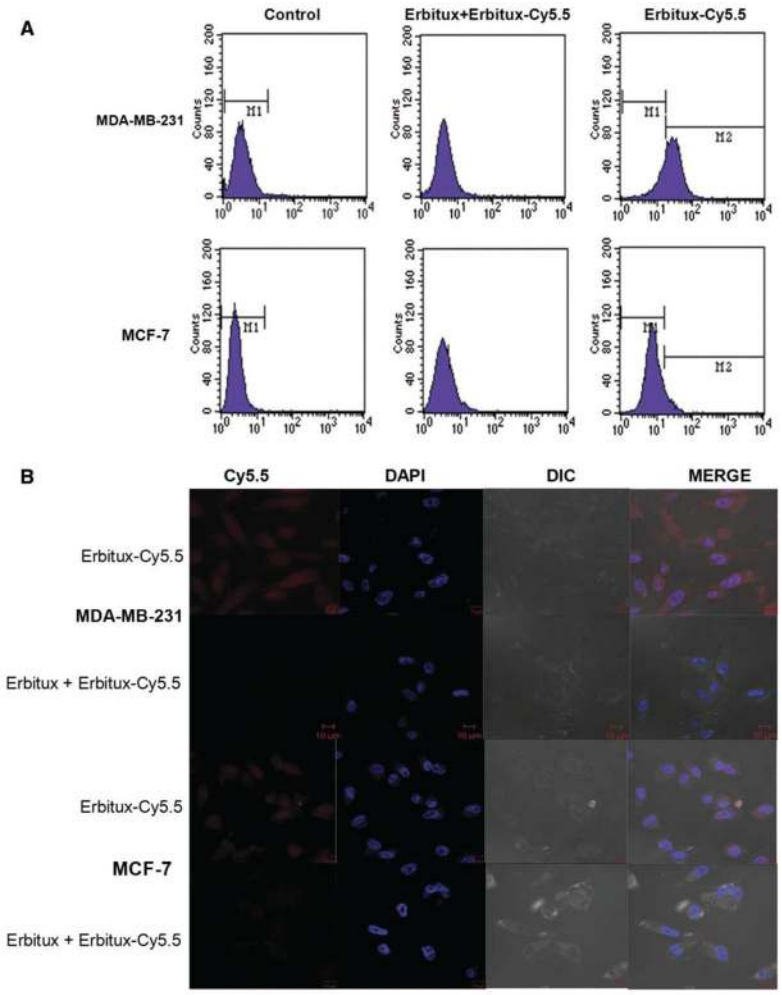

Fig. 1.

In vitro probe binding studies by flow cytometry and confocal microscopy. A. Flow cytometry results for MDA-MB-231 and MCF-7 cell lines incubation with ligand linked to a fluorescent dye. Five nM Erbitux-Cy5.5 showed strong binding to EGFR-overexpressing MDA-MB-231 cells and weak binding to low-EGFR-expressing MCF-7 cells. B. Confocal differential interference contrast (DIC) and fluorescence images of MDA-MB-231 and MCF-7 cells in the presence of Erbitux-Cy5.5. The first and third rows display the results from the cells incubated with 5 nM Erbitux-Cy5.5. The second and fourth rows display cells pretreated with Erbitux before incubation with Erbitux-Cy5.5. All images were acquired under the same conditions and are displayed on the same scale (scale bar, 10 μm).

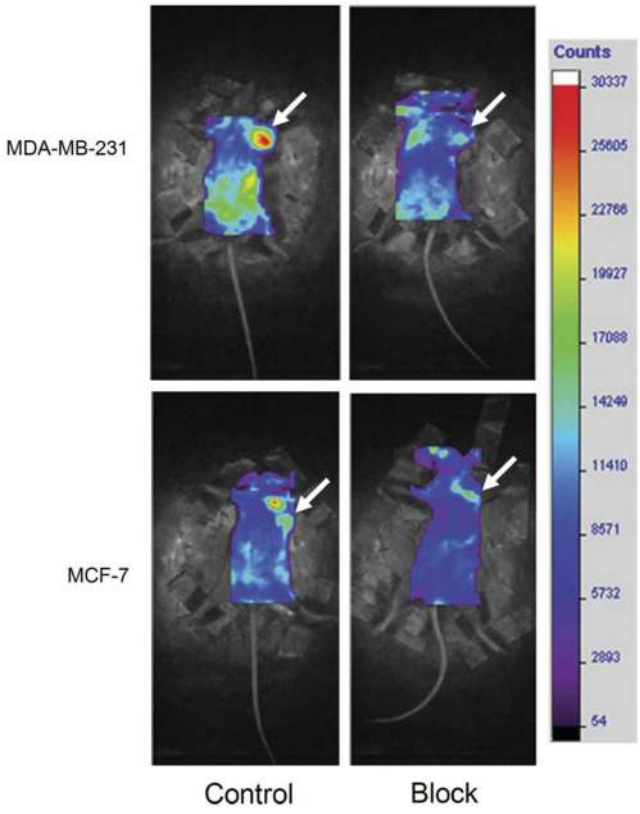

Fig. 2.

In vivo near-infrared (NIR) imaging. MDA-MB-231 or MCF-7 cells were injected into the left chest mammary gland fat pad of female athymic nude mice. Representative whole-body NIR images of MDA-MB-231 and MCF-7 xenograft mice at 24 hours post injection of Erbitux-Cy5.5 are shown. Fluorescence signal is clearly visualized in the left thoracic tumor region of MDA-MB-231 and MCF-7 xenografts. Blocking experiment indicates an apparent decrease of fluorescent signals by pre-injection of excess Erbitux (tumors indicated by arrows).

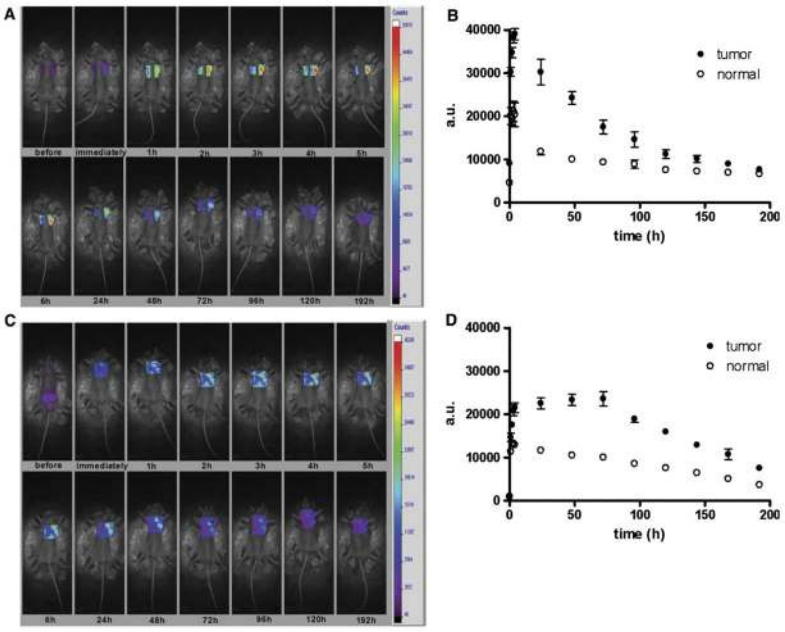

Fig. 3.

In vivo probe kinetics comparison in MDA-MB-231 and MCF-7 tumor models. Fluorescence intensity in the tumor regions after injection of Erbitux-Cy5.5 in mice with MDA-MB-231 tumors (A) and with MCF-7 tumors (C) was significantly higher than that in normal regions (P <0.001) and changed with time (P <0.001 both for MDA-MB-231 and MCF-7, B and D). In mice with MDA-MB-231 tumors, the rate of Erbitux-Cy5.5 uptake was higher than that of MCF-7 tumors, with maximum probe uptake dose 1.65-fold higher in MDA-MB-231 than MCF-7 tumors (P <0.001). All plots are representative of results from the group of mice treated under the same experimental conditions (n = 5/group).

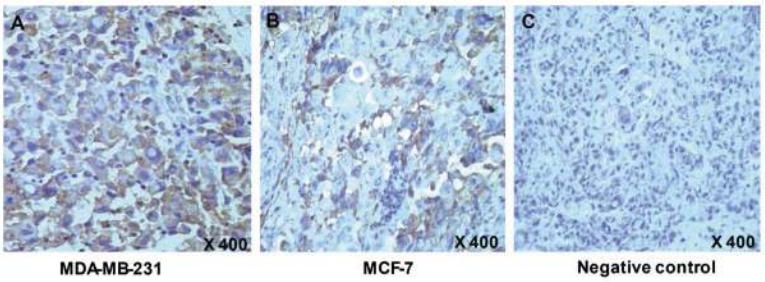

Fig. 4.

EGFR immunohistochemical assay. A. The strong red-brownish membrane-bound immunostaining on the tumor cells reflects the abundance of EGFR in MDA-MB-231 (+ + +) (400×). B. The moderate brownish membrane of the MCF-7 tumor cells reflects weak-to-normal EGFR expression (+) (400×). C. Negative EGFR expression control showed no membranous staining (−) (400×).